

A RE-INTERPRETATION OF *STEREO*/STE OBSERVATIONS AND ITS CONSEQUENCES

This article has been downloaded from IOPscience. Please scroll down to see the full text article.

2009 ApJ 694 L79

(<http://iopscience.iop.org/1538-4357/694/1/L79>)

[The Table of Contents](#) and [more related content](#) is available

Download details:

IP Address: 128.32.147.236

The article was downloaded on 11/03/2010 at 19:46

Please note that [terms and conditions apply](#).

A RE-INTERPRETATION OF *STEREO*/STE OBSERVATIONS AND ITS CONSEQUENCES

K. C. HSIEH¹, P. C. FRISCH², J. GIACALONE³, J. R. JOKIPII³, J. KÓTA³, D. E. LARSON⁴, R. P. LIN⁴, J. G. LUHMANN⁴,
AND LINGHUA WANG⁴

¹ Department of Physics, University of Arizona, Tucson, AZ, USA

² Department of Astronomy, University of Chicago, IL, USA

³ Department of Planetary Sciences, University of Arizona, AZ, USA

⁴ Space Sciences Laboratory, University of California, Berkeley, CA, USA

Received 2008 December 12; accepted 2009 February 6; published 2009 March 3

ABSTRACT

We present an alternate interpretation of recent *STEREO*/STE observations which were attributed to energetic neutral atoms (ENAs) from the heliosheath. The inferred ENA intensities, as a function of longitude, are very similar to the instrument response, implying that the source or sources are quite narrow. Such narrow sources may be quite difficult to ascribe to the available sources of ENAs, such as the charge exchange of energetic charged particles with ambient neutrals, which tend to be much broader. We point out that the largest intensity maximum observed by *STEREO*/STE is centered at the same ecliptic longitude as the brightest known X-ray source, Sco X-1. If this is indeed the source of the detected flux, it naturally accounts for the small source width. We find that the observed energy spectrum and intensity are also consistent with the X-rays from Sco X-1. If this interpretation is correct, then observers must take care in analyzing ENA data based on detectors sensitive to radiation other than ENAs. The problem of energy dissipation in the solar wind termination shock remains unsolved, while current understanding of the interaction between the solar wind and interstellar wind awaits future observations.

Key words: instrumentation: detectors – methods: data analysis – plasmas – shock waves – solar wind – stars: individual (Sco X-1)

1. INTRODUCTION

Observations of energetic neutral atoms (ENAs) from the heliosheath (the region between the heliospheric termination shock and the interface with the interstellar plasma) provide valuable constraints on the physics of the interaction of the Sun with the local interstellar medium. The recent crossings of the termination shock, first by *Voyager 1* in late 2004 (see, e.g., Decker et al. 2005; Stone et al. 2005), and more recently by *Voyager 2* in August of 2007 (see, e.g., Decker et al. 2008; Stone et al. 2008), have continued a recent surge of activity and observations of this important part of space.

Remote observations of photons provide additional information. These range from backscattered UV to radio waves. It has been known for more than a decade (Hsieh et al. 1992; Hsieh & Gruntman 1993; Hilchenbach et al. 1998) that the heliosheath is a significant source for ENAs, and that ENAs can be used to remotely observe the heliosheath. The recently launched *IBEX* is the first mission specifically intended to map the ENA emissions to study the nature of the interaction of the Sun with the local interstellar medium (McComas et al. 2004). Simulations and modeling of this interaction have been successful in accounting for many of the properties of the distant solar wind, the termination shock, and energetic particles.

Recently, Wang et al. (2008) published an analysis of data from the STE instrument on the *STEREO* mission. This instrument was designed to measure energetic electrons from the Sun, but is also sensitive to neutral atoms and other radiations (Lin et al. 2008). The instrument has low angular resolution in ecliptic latitude β , but its motion around the Sun gives it good resolution in ecliptic longitude λ . The hypothesis, in that paper, was put forth that the instrument was responding to ENAs from the heliosheath.

Roelof (2008) pointed out that the shapes of the flux peaks were quite similar to the instrumental response, and that there-

fore the sources were likely quite narrow in longitude. Here we note that the location of the larger of the two flux maxima noted by Wang et al. (2008; Figure 3) is very close to the very bright X-ray source Sco X-1 and this is very likely the source of the signal. We present arguments which support this hypothesis, and show that the energy spectrum and intensity are also in agreement with this interpretation. We suggest that the secondary flux maximum is caused by other X-ray sources near the galactic plane.

2. THE HYPOTHESIS OF AN X-RAY SOURCE

In the following, “ref. A” stands for “Wang et al. (2008)” and “ref. B” for “Lin et al. (2008),” since we will be referring to them often.

In this section, instead of interpreting the flux measured by STE-D as ENAs coming from the heliosheath, we examine the cause of the narrowness of the observed flux peaks reported in ref. A.

When scanning a radiation field with a detector, the measured angular distribution of the flux is the convolution of the angular spread of the source and the angular response function of the instrument. Only for a distant point source, represented by a Dirac delta function, will the measured distribution reproduce the response function. When the full width at half maximum (FWHM) of the two measured flux peaks in ecliptic longitude ($\Delta\lambda \approx 20^\circ$) is comparable to the 30° field of view (FOV) of the individual detectors in the ecliptic, a closer look at the detector’s angular response function is warranted.

We examine the angular response curve of D3 of STE-D in the ecliptic, because D3 of STE-D on *STEREO B* shows the clearest structure of the major flux peak afforded by the longest period of low solar wind electron flux. Hence we examine its angular response curve in the ecliptic (see Figures 1 and 2 of ref. A, also Figure 1 here). Each detector has a sensitive area $A_o =$

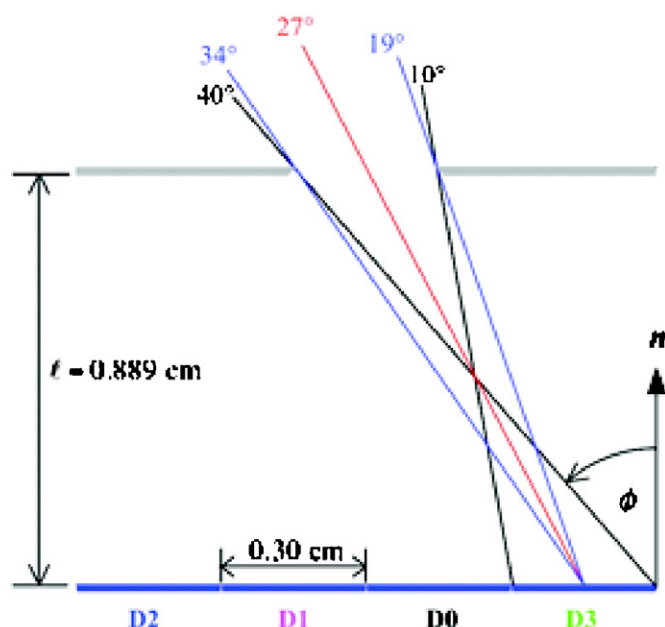


Figure 1. Sketch showing the detector aperture geometry of STE-D in the ecliptic plane, also the mid-plane of the system (see Figure 2 of Lin et al. 2008). Each of the four detectors has area 0.09 cm^2 . The aperture has dimensions 0.3 cm by 1.22 cm , oriented normal to the page. Detectors D2 and D3 each have geometrical factor $0.021 \text{ cm}^2 \text{ sr}$. The entire system has a geometrical factor $0.10 \text{ cm}^2 \text{ sr}$ (Lin et al. 2008).

$(0.3)^2 \text{ cm}^2$ and their shared rectangular aperture has dimensions 0.3 cm by 1.23 cm , the same as the four-detector array, but lying parallel to the detector plane and rotated 90° about the central axis connecting the center of the aperture and the center of the detector array. The separation of the two planes is 0.889 cm . Ignoring latitudinal effects—to be justified later—the angular response of D3 in the ecliptic is directly proportional to its exposed area projected normal to the incident beam from a given direction. With this geometry, D3 has a 30° FOV in the ecliptic spanning over $\phi = [10^\circ, 40^\circ]$, a triangular response function peaking at $\phi = 27^\circ$, and a geometrical factor of $0.021 \text{ cm}^2 \text{ sr}$. The slightly skewed and overlapping triangular response curves of the four detectors of STE-U are shown in Figure 7 of ref. B.

The one-dimensional response function of D3 and the angular distribution of the major flux peak measured by D3 of STE-D on *STEREO B* are compared in Figure 2, after normalizing the two sets to their respective maximum values for convenience. The comparable angular spread in the data and the response function imply an extremely narrow source, which is currently very difficult to attribute to ENAs of heliosheath origin. The more likely interpretation is the detection of $3\text{--}15 \text{ keV}$ X-rays from a point source located near $\lambda = 246^\circ$. The bright and variable X-ray binary Sco X-1, conveniently located at ecliptic coordinates $\lambda = 245.8^\circ$ and $\beta = 5.7^\circ$, becomes the convincing candidate. The low β of Sco X-1 and STE-D's 80° FOV in latitude justify our ignoring any latitudinal effects in considering the response function.

To further investigate Sco X-1 as the alternative source of the major flux peak detected by *STEREO*, we plotted (crosses in Figure 2) the normalized $15\text{--}50 \text{ keV}$ X-ray flux *STEREO* would have detected as D3 scans the ecliptic longitude range $245^\circ\text{--}260^\circ$ and Sco X-1 transits its FOV from 2007 DOY 159 to 188. The X-ray fluxes used in this convolution are the daily averages for the said time interval, based on data from

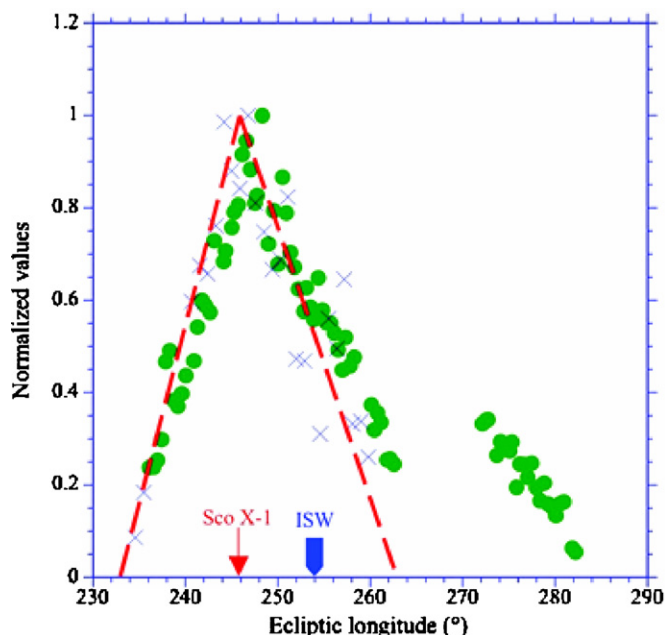


Figure 2. Observed angular distributions and the angular response of D3 of STE-D in the ecliptic. The dots are normalized 6.8 keV “ENA” flux detected by D3 on *STEREO B* as a function of ecliptic longitude (Wang et al. 2008). Overlaid is the normalized response curve of D3 (see similar curves for STE-U in Figure 7 of Lin et al. (2008)). The peak of this response function is set at the location of Sco X-1, $\lambda = 245.8^\circ$. The crosses are normalized $15\text{--}50 \text{ keV}$ X-ray flux, which *STEREO* would have seen as Sco X-1 transits D3's FOV. This convolution used the daily averages based on *Swift*/BAT data (<http://heasarc.gsfc.nasa.gov/docs/swift/results/transients/>). The similarity between the two datasets strongly suggests that the “ENA” flux may well be X-ray flux from Sco X-1. The deviations between the two sets and among the fluxes detected by the other detectors of STE-D are discussed in this Letter. The receding portion of the minor peak between $\lambda = (272^\circ, 283^\circ)$ shows a negative slope similar to that of the major peak, hence also suggesting X-ray sources in view. The direction of the interstellar wind is shown at $\lambda = 254^\circ$.

<http://heasarc.gsfc.nasa.gov/docs/swift/results/transients/>. The two data sets (dots and crosses) deviate from the triangular response function with a similar trend, even though the two sets are not congruent. These variances can be understood in the context of the highly variable light curves of Sco X-1, a low-mass X-ray binary, and in *Swift*/BAT's data coverage. Abrupt changes in Sco X-1's X-ray emission have durations ranging from minutes to weeks, but the corresponding light curves for the different bandpasses in the range $1.3\text{--}20 \text{ keV}$ are correlated (McNamara et al. 1998). Because of the frequent short-term variations, unless *STEREO* and *Swift*/BAT had identical observation times, the two data sets cannot track each other. This deviation is worsened by the fact that the daily averages are based on varied data coverage, e.g., on DOY 169 (corresponds to $\lambda = 243^\circ$ in Figure 2) *Swift*/BAT had more than 20 pointings with fluxes differing by a factor of 7, while on DOY 180 (corresponds to $\lambda = 253^\circ$ in Figure 2) there was only one pointing with a low flux. In view of these facts, the resemblance of the longitudinal distribution of the peaked “ENA” flux to that of the convolved X-ray flux from Sco X-1 strongly suggests Sco X-1 as the source of the major flux peak detected by *STEREO*. The variations among the measurements of the same flux peak by the different STE-D detectors on *STEREO* over time are consistent with this interpretation.

The extremely low-noise solid-state detectors used in STE are excellent X-ray detectors (Figure 5 of Tindall et al. 2008 and ref. B); but can Sco X-1 produce the flux and spectral shape detected by STE-D on *STEREO A* and *B*?

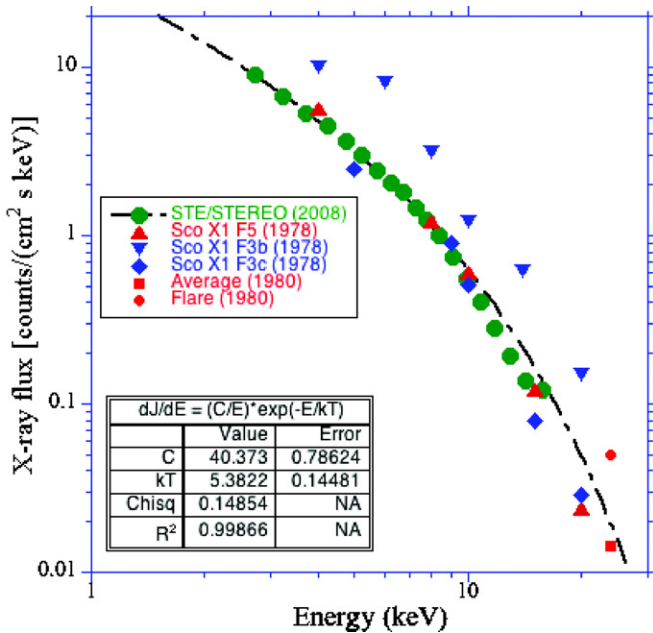


Figure 3. Comparing the spectrum detected by STE-D/*STEREO* A and B from the major peak centered at $\lambda \approx 246^\circ$, after treating the flux as due to X-rays, with some published Sco X-1 X-ray spectra. The STE spectrum was obtained by averaging *STEREO* A observation over $\lambda = [241^\circ, 252^\circ]$ and *STEREO* B observations over $\lambda = [238^\circ, 249^\circ]$. The detector's X-ray calibration and geometrical factor have been used in constructing the spectrum as that of X-rays. Data marked (1978) are taken, respectively, from Figures 3(b), 3(c), and 5 of Miyamoto et al. (1978). The two data points at 24 keV are from Rothschild et al. (1980). Sco X-1's X-ray emission is variable, as evident in this figure. This would explain the variations shown in Figure 2 and in Wang et al. (2008). The STE-D measurement is averaged over a period of time (Wang et al. 2008). The model fit to the STE-D data gives a temperature of 5.38 keV, not far from the range reported in the two references cited above.

Re-analyzing the data collected by D3 of STE-D on *STEREO* A in ecliptic longitudes $\lambda = [241^\circ, 252^\circ]$ and on *STEREO* B in $\lambda = [238^\circ, 249^\circ]$ associated with the major flux peak assuming X-rays instead of ENAs produces a time-averaged spectrum which can be compared with the known X-ray spectra of Sco X-1. In conversion from flux in “counts/(cm² sr s keV)” to a unidirectional flux in “counts/(cm² s keV),” the average geometrical factor of 0.025 cm² sr for the four detectors is used. The energy designations of the data points are now based on the average response of the four detectors to X-rays.

The re-interpreted STE-D measured spectrum of the major flux peak is compared with some published Sco X-1 X-ray spectra in Figure 3. The X-ray spectra are taken from Miyamoto et al. (1978) and Rothschild et al. (1980). The model fit to Bremsstrahlung in thermal equilibrium with the stellar plasma, $dj/dE = (C/E) \exp(-E/kt)$, yields a temperature of 5.38 keV, which is not far from the range of temperature 2.5 keV (Miyamoto et al. 1978) to 5.15 keV (Rothschild et al. 1980), since Sco X-1 is a variable source. This would explain the variations between the flux and the response function shown in Figure 2 and among the fluxes registered by the different detectors at different times (ref. A).

The arguments presented above, based on the angular spread of the major flux peak, the flux level, and spectra shape, suggest strongly that X-rays coming from Sco X-1 is the preferred interpretation for the major flux peak.

3. DISCUSSION AND CONCLUSIONS

Noting the narrow width observed for the heliosheath ENA sources discussed in ref. A, we have presented an

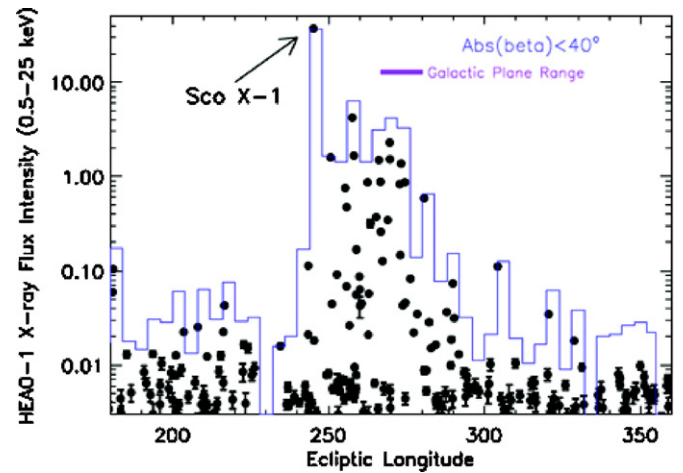


Figure 4. Brightest X-ray sources from the all-sky HEAO-1 survey (Wood et al. 1984). The flux units represent the apparent intensity of the source in counts cm⁻² s⁻¹ for photons in the range 0.5–25 keV within $\pm 40^\circ$ of the ecliptic latitude β , the FOV of STE-D. The blue histogram is the sum of the point source fluxes, including point sources with fluxes below the 0.003 cutoff in the plot Y-axis.

alternate interpretation. We have demonstrated that the larger of the two peaks is consistent with it being caused by the X-ray source Sco X-1, which would produce a narrow peak in flux at about the correct location. Moreover, the intensity and energy spectrum are also consistent with this interpretation. Since producing such a narrow source using charge exchange of energetic charged particles and ambient neutral hydrogen is difficult, we feel that this identification is favored.

Judging from the shape of the minor peak at $\lambda \approx 270^\circ$, especially the negative slopes at higher λ , we believe this peak is also due to X-ray sources. As Figure 4 shows, there are a number of X-ray sources in the ecliptic longitude range of $\lambda = (260^\circ, 290^\circ)$, including those in the Galactic center, but none of them alone are bright enough to account for the flux measured in the minor peak. We tentatively identify GX5-1 at $\lambda = 269^\circ$ and $\beta = -1^\circ$, Sgr X4 at $\lambda = 275^\circ$ and $\beta = -7^\circ$, and others shown in Figure 4, as the combined source producing the minor peak. More detailed work will be needed to resolve the minor peak. We note that Collier et al. (2004) reported a similar low-energy ENA flux peak centered around $\lambda \approx 270^\circ$ (their Figure 4), which takes the shape of a skewed triangle with straight sides and a base, i.e. at zero flux, of ≈ 90 days or $\Delta\lambda \approx 90^\circ$.

From the experimentalist point of view, this exercise cautions us that X-rays are another background noise we have to deal with. For ENA instruments with triple coincidence, such as in HSTOF of *CELIAS*/SOHO (Hovestadt et al. 1995), *HENA*/IMAGE (Mitchell et al. 2000), and *IBEX* (McComas et al. 2004), X-ray should not be a concern. It is very important to remember that all ENA images are like photon images in that they are convolutions of the source function and the instrument response function. Therefore, all observed angular distributions must be deconvolved prior to meaningful analysis.

This re-interpretation of the *STEREO* observations has consequences for the physics of the termination shock and heliosheath. The problem of the energy dissipated in the termination shock, suggested by Wang et al. (2008) on the basis of their original interpretation of the data, remains unsolved. Understanding of the dynamics and morphology of the heliosheath in the direction of interstellar flow remains as previously understood (e.g., Czechowski et al. 2008).

We thank R. E. Rothschild for useful suggestions and the *Swift*/BAT team for their help in using their data. This work at the University of Arizona was supported by NSF under grant ATM0447354 and by NASA under grants NNG05GE83G and NNX07AH19G, and contract NAS5-97271 subcontracted through Johns Hopkins University. The work at the University of California was supported under NASA grant NAS5-03131.

REFERENCES

- Collier, M. R., et al. 2004, *Adv. Space Res.*, **34**, 166
- Czechowski, A., Hilchenbach, M., Hsieh, K. C., Grzedzielski, S., & Kóta, J. 2008, *A&A*, **487**, 329
- Decker, R. B., Krimigis, S. M., Roelof, E. C., Hill, M. E., Armstrong, T. P., Gloeckler, G., Hamilton, D. C., & Lanzerotti, L. J. 2005, *Science*, **309**, 2020
- Decker, R. B., Krimigis, S. M., Roelof, E. C., Hill, M. E., Armstrong, T. P., Gloeckler, G., & Hamilton, D. C. 2008, *Nature*, **454**, 67
- Hilchenbach, M., et al. 1998, *ApJ*, **503**, 916
- Hovestadt, D., et al. 1995, *Sol. Phys.*, **162**, 441
- Hsieh, K. C., & Gruntman, M. A. 1993, *Adv. Space Res.*, **33**, 131
- Hsieh, K. C., Shih, K. L., Jokipii, J. R., & Grzedzielski, S. 1992, *ApJ*, **393**, 756
- Lin, R. P., et al. 2008, *Space Sci. Rev.*, **136**, 241
- McComas, D., et al. 2004, in AIP Conf. Proc. 719, Physics of the Outer Heliosphere: 3rd Annual IGPP Conference, ed. V. Florinski, N. V. Pogorelov, & G. P. Zank (New York: AIP), 162
- McNamara, R. J., Harrison, T. E., Mason, P. A., Templeton, M., Heikkila, C. W., Buckley, T., Galvan, E., Silva, A., & Harmon, B. A. 1998, *ApJS*, **116**, 287
- Mitchell, D. G., et al. 2000, *Space Sci. Rev.*, **91**, 67
- Miyamoto, S., Matsuoka, M., Oda, M., & Ogawara, Y. 1978, *A&A*, **65**, 329
- Roelof, E. C. 2008, Talk Presented at the Huntsville Workshop "The Physical Processes for Energy and Plasma Transport across Magnetic Boundaries," Huntsville, AL
- Rothschild, R. E., et al. 1980, *Nature*, **286**, 786
- Stone, E. C., Cummings, A. C., Mc Donald, F. B., Heikkila, B. C., Lal, N., & Webber, W. R. 2005, *Science*, **309**, 2017
- Stone, E. C., Cummings, A. C., McDonald, F. B., Heikkila, B. C., Lal, N., & Webber, W. R. 2008, *Nature*, **454**, 71
- Tindall, C. S., et al. 2008, *IEEE Trans. Nucl. Sci.*, **55**, 797
- Wang, L., Lin, R. P., Larson, D. E., & Luhmann, J. G. 2008, *Nature*, **454**, 81
- Wood, K. S., et al. 1984, *ApJS*, **56**, 507